AGU PUBLICATIONS

Geophysical Research Letters

RESEARCH LETTER

10.1002/2016GL071275

Key Points:
- Overall atmospheric winds significantly damp ocean eddies
- The large-scale wind stress curl systematically strengthens or weakens ocean eddies
- There is a linear relationship between the wind stress curl and wind work on eddies

Supporting Information:
- Supporting Information S1

Correspondence to:
X. Zhai and X.-D. Shang,
xiaoming.zhai@uea.ac.uk;
xdshang@scsio.ac.cn

Citation:
Xu, C., X. Zhai, and X.-D. Shang (2016), Work done by atmospheric winds on mesoscale ocean eddies, *Geophys. Res. Lett.*, *43*, 12,174–12,180, doi:10.1002/2016GL071275.

Received 20 SEP 2016
Accepted 13 NOV 2016
Accepted article online 17 NOV 2016
Published online 2 DEC 2016

Work done by atmospheric winds on mesoscale ocean eddies

Chi Xu[1,2], Xiaoming Zhai[2], and Xiao-Dong Shang[1]

[1]State Key Laboratory of Tropical Oceanography, South China Sea Institute of Oceanology, Chinese Academy of Sciences, Guangzhou, China, [2]Centre for Ocean and Atmospheric Sciences, School of Environmental Sciences, University of East Anglia, Norwich, UK

Abstract Mesoscale eddies are ubiquitous in the ocean and dominate the ocean's kinetic energy. However, physical processes influencing ocean eddy energy remain poorly understood. Mesoscale ocean eddy-wind interaction potentially provides an energy flux into or out of the eddy field, but its effect on ocean eddies has not yet been determined. Here we examine work done by atmospheric winds on more than 1,200,000 mesoscale eddies identified from satellite altimetry data and show that atmospheric winds significantly damp mesoscale ocean eddies, particularly in the energetic western boundary current regions and the Southern Ocean. Furthermore, the large-scale wind stress curl is found to on average systematically inject kinetic energy into anticyclonic (cyclonic) eddies in the subtropical (subpolar) gyres while mechanically damps anticyclonic (cyclonic) eddies in the subpolar (subtropical) gyres.

1. Introduction

Eddies play a vital role in shaping the large-scale ocean circulation and in transporting mass, heat, and other climatically important tracers in the ocean [e.g., *Gill et al.*, 1974; *Hecht and Smith*, 2008]. Although progress has been made in recent years [e.g., *Wunsch*, 1998; *Zhai et al.*, 2010; *Nikurashin et al.*, 2012], our understanding of physical processes governing eddy energy in the ocean remains rather limited. One of the physical processes that may have a significant impact on ocean eddies and the energy they carry, but yet to be quantified, is mesoscale eddy-wind interaction, i.e., direct work done by the wind on ocean eddies.

It has been recognized [e.g., *Dewar and Flierl*, 1987; *Duhaut and Straub*, 2006; *Dawe and Thompson*, 2006; *Zhai and Greatbatch*, 2007; *Hughes and Wilson*, 2008; *Scott and Xu*, 2009; *Zhai et al.*, 2012] that atmospheric winds can systematically damp the ocean currents if the relative motion between the atmosphere and underlying surface ocean is taken into account in the surface stress calculation (so-called "relative wind stress effect"). Because the eddies dominate kinetic energy at the ocean surface, simple scaling analysis suggests that damping by the relative wind stress should primarily operate on mesoscale eddies [*Duhaut and Straub*, 2006; *Hughes and Wilson*, 2008]. Reduction in wind power input to the ocean when the relative wind stress is used in the power calculation is therefore generally attributed to the negative wind work on ocean eddies [*Hughes and Wilson*, 2008; *Zhai et al.*, 2012]. However, to our knowledge, there have been no direct observational studies yet that clearly demonstrate and quantify the damping effect of ocean eddies by the relative wind stress, particularly on a global scale.

Since atmospheric winds tend to vary on much greater spatial scales than mesoscale ocean eddies, interpretation of eddy-wind interaction often assumes that the background wind field is spatially uniform over the lateral extent of the eddies and therefore generally emphasizes the vortex structure of ocean eddies and its role in generating the anomalous relative wind stress curl on the scale of the eddies [*Duhaut and Straub*, 2006; *Zhai and Greatbatch*, 2007; *Zhai et al.*, 2012]. On the other hand, it is well known that the surface wind stress exhibits large spatial variations characterized by anticyclonic wind stress curl in the subtropical ocean and cyclonic wind stress curl in the subpolar ocean (see Text S1 in the supporting information). Little is known about the impact of the large-scale wind stress curl on power input to mesoscale ocean eddies. Here we use satellite observations to quantify for the first time the work done by atmospheric winds on mesoscale eddies in the global ocean.

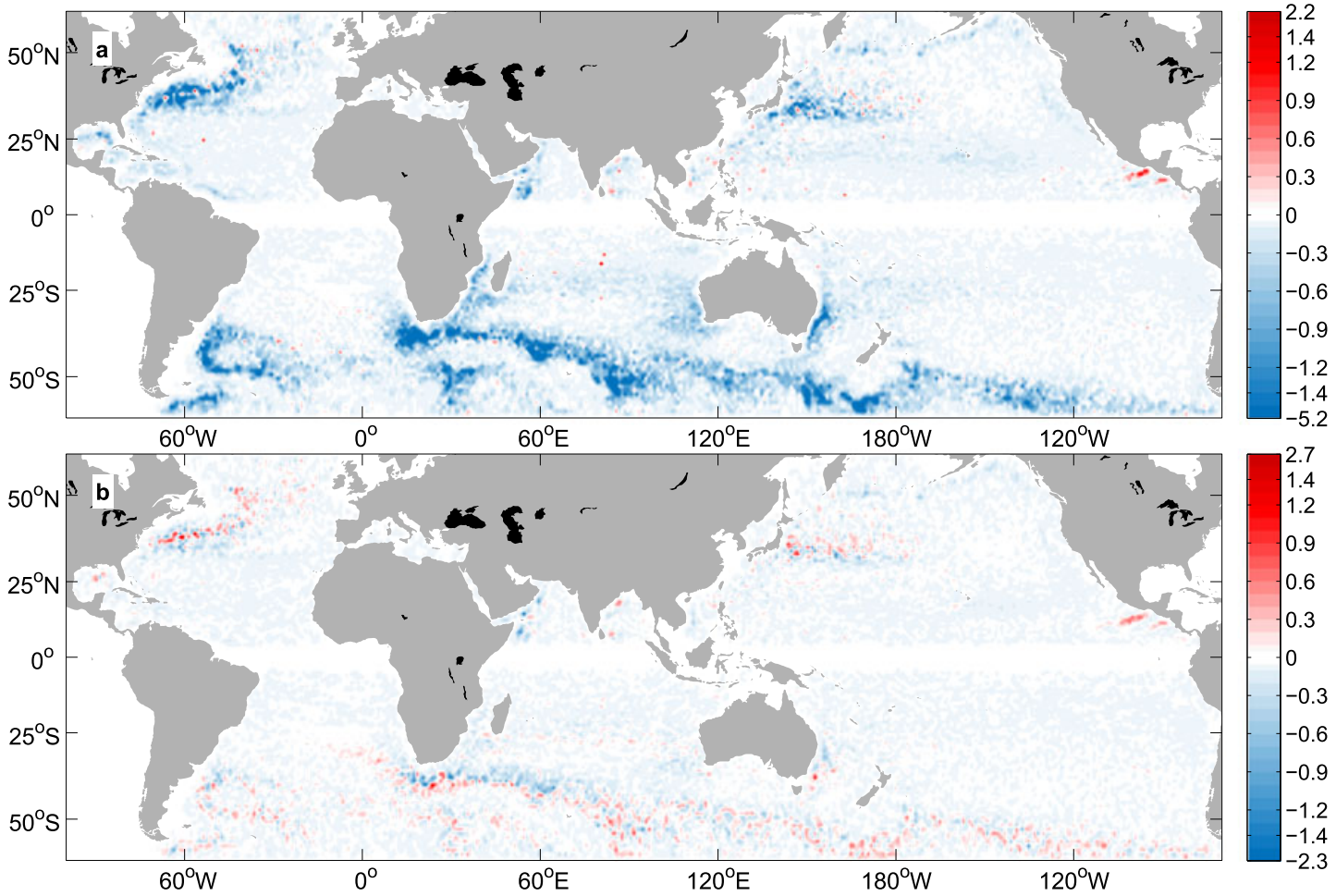

Figure 1. Wind work on mesoscale ocean eddies. (a) Work done (mW m^{-2}) by atmospheric winds on mesoscale eddies calculated from the combination of altimetry and scatterometer data and averaged over the period from July 1999 to November 2009. (b) The same as Figure 1a except that the spatially filtered scatterometer wind stress is used in the power calculation.

2. Data and Method

Our analysis starts with the identification of 1,247,166 ocean eddies from weekly maps of satellite-derived sea level anomalies (SLA) [*Ducet et al.*, 2000] over a period of approximately 10 years (July 1999 to November 2009). The weekly SLA fields used here are obtained from Archiving, Validation, and Interpretation of Satellite Data in Oceanography (AVISO). These SLA data are constructed by merging Topex/Posiden, *Jason-1*, or *Jason-2* measurements with ERS-1, ERS-2, or ENVISAT and are provided at a spatial resolution of 0.25° × 0.25°. In this study the eddies are detected based on closed contours of sea level anomalies following the method developed by *Chelton et al.* [2011] (see Appendix A for details).

Daily QuikSCAT scatterometer wind stress fields [*Risien and Chelton*, 2008] over the period of 19 July 1999 to 23 November 2009 are used for wind power calculation. The QuikSCAT wind stress data are provided on a 0.25° × 0.25° grid over the global ocean. For each eddy detected, we collocate the simultaneous QuikSCAT scatterometer wind stress measurements and then calculate wind power input to each individual eddy using $\boldsymbol{\tau} \cdot \mathbf{u}_s$, where $\boldsymbol{\tau}$ is the scatterometer wind stress and $\mathbf{u}_s$ is the eddy surface geostrophic velocity derived from sea level anomalies. In order to separate work done by the large-scale wind stress curl from damping of eddies by the relative wind stress, we repeat the calculation of wind power input to mesoscale eddies using the spatially filtered scatterometer wind stress where the small-scale features in the wind stress owing to the presence of ocean surface currents are removed (see Appendix B). Therefore, the damping effect of the relative wind stress is effectively eliminated in the second power calculation. Note that some of the small-scale features in the wind stress field are associated with mesoscale air-sea thermodynamic coupling, but the effect of thermodynamic

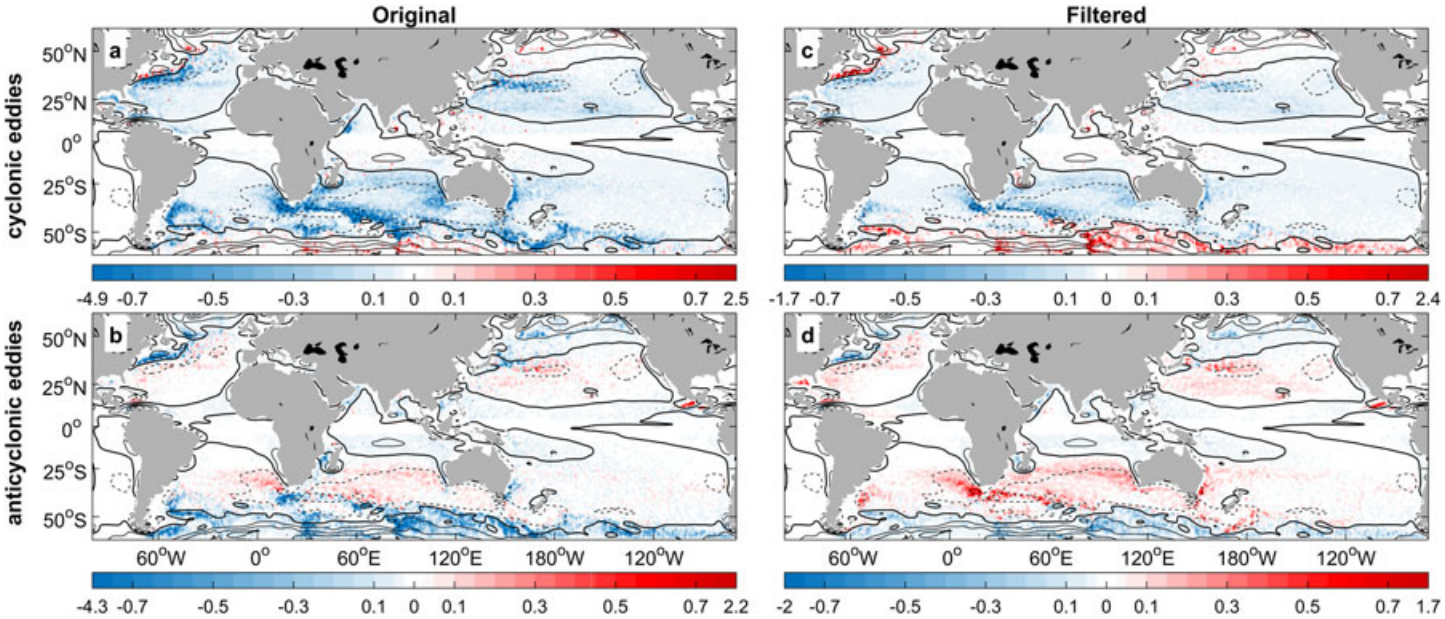

Figure 2. Wind work on cyclonic and anticyclonic ocean eddies. Work done (mW m^{-2}) by atmospheric winds on (a) cyclonic and (b) anticyclonic eddies calculated from the combination of altimetry and scatterometer data and averaged over the period from July 1999 to November 2009. (c and d) The same as Figures 2a and 2b except that the spatially filtered scatterometer wind stress is used in the power calculation. The thick black contour marks the zero climatological wind stress curl calculated from the spatially filtered scatterometer wind stress (N m^{-3}). The solid and dashed thin black contours are contours of cyclonic and anticyclonic wind stress curl, respectively, with an interval of 10^{-7} N m^{-3}. Note the different color scale from Figure 1.

coupling on wind work on ocean eddies is generally considered to be of secondary importance [e.g., *Gaube et al.*, 2015]. Potential errors and uncertainties associated with the method and data used in this study are discussed in Appendix C.

3. Results

Figure 1a shows the work done by atmospheric winds on mesoscale ocean eddies calculated from the combination of altimetry and scatterometer data and averaged over the 10 year study period (see Appendix D for details of wind work map generation). The wind work on mesoscale eddies is almost everywhere negative, consistent with the idea of relative wind stress damping of ocean eddies. The most significant negative wind work is found in the western boundary current regions and in the Southern Ocean where the atmospheric and oceanic storm tracks coincide. This is in agreement with the theoretical prediction [*Duhaut and Straub*, 2006]: damping by the relative wind stress is proportional to both the wind speed and ocean surface kinetic energy. Furthermore, the spatial pattern of wind work on mesoscale eddies is very similar to that of the reduction in wind power input to the ocean general circulation when the relative wind stress is used in the power calculation [e.g., *Hughes and Wilson*, 2008; *Zhai et al.*, 2012]. Integrated over the ocean between 60°N and 60°S, the net work done by atmospheric winds on mesoscale ocean eddies is about −27.7 GW (1 GW = 10^9 W), which is comparable to previous estimates of the time-dependent component of wind work away from the tropics [*Hughes and Wilson*, 2008] (∼−30 GW). In comparison, the net work done on mesoscale eddies by the spatially filtered scatterometer wind stress is indistinguishable from zero (Figure 1b) owing to the absence of damping by the relative wind stress.

To investigate the role of the large-scale wind stress curl in energy input to mesoscale eddies in the ocean, we now consider wind work on cyclonic and anticyclonic eddies separately. Maps of wind work on cyclones and anticyclones reveal striking large-scale patterns of positive and negative wind work delineated by the contours of zero wind stress curl (Figures 2a and 2b). The wind field generally injects kinetic energy into the anticyclones in the subtropical gyres and cyclones in the subpolar gyres where the background wind stress curl is in the same direction as these eddies, while it damps the cyclones in the subtropical gyres and anticyclones in the subpolar gyres where the background wind stress curl is in the opposite direction to these eddies (see supporting information Texts S1 and S2). Integrated over the subtropical gyres (defined as regions of climatological anticyclonic wind stress curl enclosed by the thick black contours in Figure 2), the total wind work

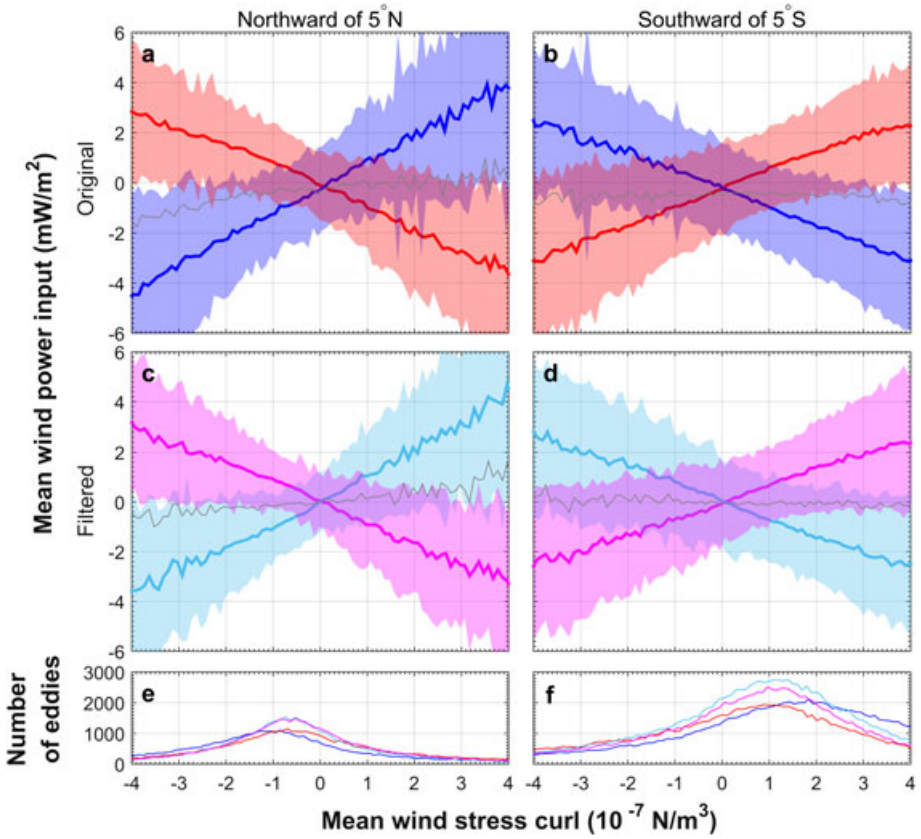

Figure 3. Wind work on cyclones and anticyclones as a function of the wind stress curl. (a and b) Average wind work (mW m^{-2}) on cyclones (thick blue), anticyclones (thick red), and both types of eddies (thin grey) in the Northern Hemisphere and Southern Hemisphere, respectively. Color shading represents the standard deviation. (c and d) The same as Figures 3a and 3b except that the spatially filtered scatterometer wind stress is used in the power calculation. (e and f) The number of cyclones and anticyclones as a function of the wind stress curl. The line colors used in Figures 3e and 3f are the same as in Figures 3a–3d, i.e., blue (cyan) for cyclones and red (magenta) for anticyclones when the original (filtered) wind stress is used. The wind stress curl is first averaged over the area of each eddy and then binned into intervals with a width of 0.1×10^{-7} N m^{-3}. The mean wind work is obtained by averaging wind work on eddies that have their mean wind stress curl in the same bin.

on cyclones and anticyclones is -20.6 ± 4.1 GW and 0.3 ± 3.8 GW, respectively. In contrast, the work done by the spatially filtered scatterometer wind stress on both cyclones and anticyclones appears more positive everywhere owing to the absence of damping by the relative wind stress (Figures 2c and 2d). However, the overall pattern of wind work remains unchanged, demonstrating that it is the large-scale background wind stress curl, not the curl associated with the relative wind stress, that is the cause of these large-scale patterns of positive and negative wind work on cyclones and anticyclones. Integrated over the subtropical gyres, the total work done by the spatially filtered wind stress on cyclones and anticyclones is -8.8 ± 3.0 GW and 7.7 ± 2.7 GW, respectively, comparable in magnitude to the net damping effect of the relative wind stress in the subtropical gyres (-11.8 ± 2.5 GW for cyclones and -7.4 ± 2.0 GW for anticyclones).

To further quantify the relationship between the curl of surface wind stress and wind work on mesoscale eddies, we compute the average wind work on cyclones and anticyclones in both hemispheres as a function of the wind stress curl (Figures 3a and 3b). Several interesting features emerge. First, the average wind work on both cyclones and anticyclones varies linearly with the strength of the wind stress curl that the eddies are subject to. This linear relationship can be understood by the following simple example. Suppose that a circular anticyclonic eddy with a radius of R and rotational speed of u_s is subject to a zonal wind stress that varies in the meridional direction with $\alpha = \partial\tau/\partial y$. It can be easily shown (see supporting information Text S3) that the net wind work on this eddy is proportional to the magnitude of the imposed wind stress curl and is given by $\pi\alpha u_s R^2$. Second, the relationship between the wind work and wind stress curl in Figures 3a and 3b is not symmetric about zero but shifted as a whole toward negative values of wind work. For example, the red, blue,

and grey lines do not pass through the origin. This is, again, due to the damping effect of the relative wind stress, as this asymmetry disappears when the spatially filtered scatterometer wind stress is used in the power calculation (Figures 3c and 3d). Finally, the majority of the eddies identified from satellite altimetry data in our study are found to live in regions of anticyclonic wind stress curl (Figures 3e and 3f), where the anticyclones are preferentially enhanced and cyclones suppressed.

4. Discussion

Work done by atmospheric winds on mesoscale ocean eddies could have a direct impact on eddy energetics. Damping of eddies by the relative wind stress is systematic and significant, providing a way of removing eddy energy in the ocean. Given that the global eddy energy is estimated to be in the range of 1.40–3.25 EJ (1 EJ = 10^{18} J) [*Xu et al.*, 2014], damping by the relative wind stress gives an average eddy energy spin-down time of 1.6–3.7 years. This spin-down time is longer than, but still of the same order of magnitude as, recent estimates of eddy lifetime (~8 months) from tracking eddy sea level signatures [*Chelton et al.*, 2011; *Xu et al.*, 2014], suggesting that mesoscale eddy-wind interaction can play a nonnegligible role, although may not be the dominating process, in determining the level of eddy energy in the ocean. This notion is further supported by numerical modeling studies [e.g., *Zhai and Greatbatch*, 2007; *Eden and Dietze*, 2009; *Munday and Zhai*, 2015] where the eddy kinetic energy is found to decrease by ~20% when damping by the relative wind stress is included. Our estimated eddy spin-down time owing to damping by relative wind stress is comparable to a previous estimate of ~1.3 years based on Ekman pumping argument [*Gaube et al.*, 2015] but without the need to invoke assumptions such as eddy vertical scale and random wind direction.

Work done on eddies by the large-scale wind stress curl clearly depends on the polarity of the eddies, which may have contributed to the lifetime difference between cyclones and anticyclones found in altimetry data [*Chelton et al.*, 2011]. This direct wind impact on eddy energetics could then modulate the role the eddies play in the ocean and pose potential challenges to eddy parameterizations in ocean climate models [e.g., *Gent and McWilliams*, 1990]. For example, anticyclonic eddies are known to be capable of trapping near-inertial waves via their negative relative vorticity and acting as a conduit to drain the near-inertial energy injected at the sea surface to the deep ocean [e.g., *Kunze*, 1985; *Zhai et al.*, 2005; *Jing and Wu*, 2014]. Positive wind work on anticyclones in the subtropical gyres could potentially enhance/lengthen their trapping effect and thereby enable more near-inertial energy to reach the deep ocean, contributing to the deep ocean mixing. Finally, mesoscale eddy-wind interactions could result in anomalous vertical motions in the interior of the eddies and, as a consequence, strongly modulate the eddy-induced biological productivity and carbon export [e.g., *McGillicuddy et al.*, 1998; *Gaube et al.*, 2013; *McGillicuddy*, 2015; *Song et al.*, 2015].

Appendix A: Mesoscale Eddy Identification

Our eddy identification method is based on finding the outermost closed contour of SLA that defines a compact structure, similar to the method used in *Chelton et al.* [2011], except for the slightly different criteria used here. (1) The amplitude of the eddy, that is, the difference between the SLA extremum in the eddy interior and the value of the outermost closed SLA contour, is at least 3 cm. (2) The area bounded by this closed SLA contour is at least 0.5° long in both zonal and meridional directions. (3) The distance between any pair of points within the connected region must be less than 400 km. The center of the identified eddy is then defined as the midpoint between the centroid of the area within the outermost closed SLA contour and the location of the SLA extremum. The area of the eddy is defined as the area within the outermost closed SLA contour, and the radius of the eddy is defined as the radius of a circle that has the same area as the eddy. Regions equatorward of 5° of latitude are excluded from our analysis since the eddy identification procedure performs less well there. Readers are referred to *Chelton et al.* [2011] for further discussions of the utility as well as limitation of this eddy identification procedure.

Appendix B: Spatial Filtering

The weekly SLA field is first 2-D Fourier transformed, then multiplied by a low-pass Gaussian filter function in the wave number domain, and finally retransformed back to the spatial domain using the inverse Fourier transform. The low-pass Gaussian filter function, G, is defined as

$$G(k,l) = e^{-\frac{k^2+l^2}{2\sigma^2}}, \tag{B1}$$

where (k, l) are wave numbers in the zonal and meridional directions, respectively, and σ is a measure of the spread of the Gaussian curve. Here σ is chosen to ensure that the half-power cutoff wavelength has a distance of 10° in longitude. We then subtract the low-pass-filtered SLA from the original SLA field to remove the large-scale SLA signal mainly associated with the wind forcing and surface heating/cooling before applying the eddy identification procedure. We apply the same low-pass filtering procedure to the scatterometer wind stress field to remove small-scale features associated with the presence of ocean surface currents.

Appendix C: Errors and Uncertainties

The gridded altimetry data are subject to spatial and temporal averaging, which is likely to underestimate mesoscale variability in the ocean. Our study focuses on wind work on mesoscale ocean eddies because the resolution of the available altimetry data is too coarse to resolve submesoscale variability. Altimetry data near the coast need to be treated with caution, as standard tidal and atmospheric corrections may have larger errors than those offshore. In our calculation, we have excluded regions shallower than 200 m deep.

We have applied a two-dimensional spatial filter with half-power cutoffs at a scale of 10° to the SLA field. Sensitivity tests confirm that the eddy signal is well preserved in the SLA field used for eddy detection and our results are not particularly sensitive to the scale chosen for the spatial filter as long as it is sufficiently larger than the eddy scale. The criteria used for eddy identification have an influence on the number of eddies detected, but this does not change our conclusions.

Finally, in deriving the eddy surface velocity from the SLA field, we have assumed that the eddies are in geostrophic balance. Although this is a very good assumption over most of the ocean, it introduces errors in regions where the Rossby number is not small and the eddies are strongly nonlinear [e.g., *Douglass and Richman*, 2015].

Appendix D: Wind Work Map Generation

We first divide the global ocean into 1°×1° boxes. For each box, we sum up wind work integrated over the area of the eddy whose center falls in the box on each weekly SLA map. Finally, this sum of wind work is divided by the area of the box, and the total number of weekly SLA maps over the period of 19 July 1999 to 23 November 2009 to obtain the averaged wind work on eddies. As such, the spatial maps of wind work generated in this study represent averages in time at fixed spatial locations over the 10 year period when the QuikSCAT wind stress data and AVISO SLA data overlap. Note that the method used for generating the spatial maps of wind work shown in Figures 1 and 2 does not affect the value of total wind work on mesoscale eddies.

Acknowledgments

C.X. is supported by a visiting scholarship from the Chinese Scholarship Council and by grants 41306016, LTOZZ1502, and LTOZZ1601. X.Z. acknowledges support from the School of Environmental Sciences, University of East Anglia. X.-D. Shang is supported by grants 41630970, 41376022 and 41521005. We thank Chris Wilson, David Marshall, Yihua Lin, and Xuhua Cheng for helpful discussions. The satellite altimetry data were produced by Ssalto/Duacs and formerly distributed by Aviso+ with support from CNES (ftp://ftp.aviso.oceanobs.com; now distributed by Copernicus Marine and Environment Monitoring Service). Gridded daily QuikSCAT scatterometer wind stress fields were downloaded from ftp://podaac.jpl.nasa.gov/. We thank two anonymous reviewers for their positive and constructive comments.

References

Chelton, D. B., M. G. Schlax, and R. M. Samelson (2011), Global observations of nonlinear mesoscale eddies, *Prog. Oceanogr.*, *91*, 167–216.

Dawe, J. T., and L. Thompson (2006), Effect of ocean surface currents on wind stress, heat flux, and wind power input to the ocean, *Geophys. Res. Lett.*, *33*, L09604, doi:10.1029/2006GL025784.

Dewar, W. K., and G. R. Flierl (1987), Some effects of the wind on rings, *J. Phys. Oceanogr.*, *17*, 1653–1667.

Douglass, E. M., and J. G. Richman (2015), Analysis of ageostrophy in strong surface eddies in the Atlantic Ocean, *J. Geophys. Res. Oceans*, *120*, 1490–1507, doi:10.1002/2014JC010350.

Ducet, N., P. Y. Le Traon, and G. Reverdin (2000), Global high-resolution mapping of ocean circulation from TOPEX/Poseidon and ERS-1 and -2, *J. Geophys. Res.*, *105*, 19477–19498.

Duhaut, T. H., and D. N. Straub (2006), Wind stress dependence on ocean surface velocity: Implications for mechanical energy input to ocean circulation, *J. Phys. Oceanogr.*, *36*, 202–211.

Eden, C., and H. Dietze (2009), Effects of mesoscale eddy/wind interactions on biological new production and eddy kinetic energy, *J. Geophys. Res.*, *114*, C05023, doi:10.1029/2008JC005129.

Gaube, P., D. B. Chelton, P. G. Strutton, and M. J. Behrenfeld (2013), Satellite observations of chlorophyll, phytoplankton biomass, and Ekman pumping in nonlinear mesoscale eddies, *J. Geophys. Res. Oceans*, *118*, 6349–6370, doi:10.1002/2013JC009027.

Gaube, P., D. B. Chelton, R. M. Samelson, M. G. Schlax, and L. W. O'Neill (2015), Satellite observations of mesoscale eddy-induced Ekman pumping, *J. Phys. Oceanogr.*, *45*, 104–132.

Gent, P. R., and J. C. McWilliams (1990), Isopycnal mixing in ocean circulation models, *J. Phys. Oceanogr.*, *20*, 150–155.

Gill, A. E., J. S. A. Green, and A. J. Simmons (1974), Energy partition in the large-scale ocean circulation and the production of mid-ocean eddies, *Deep-Sea. Res.*, *21*, 499–528.

Hecht, M. W., and R. D. Smith (2008), Towards a physical understanding of the North Atlantic: A review of model studies in an eddying regime, in *Ocean Modelling in an Eddying Regime, Geophys. Monogr.*, vol. 177, pp. 213–240, AGU, Washington, D. C.

Hughes, C., and C. Wilson (2008), Wind work on the geostrophic ocean circulation: An observational study on the effect of small scales in the wind stress, *J. Geophys. Res.*, *113*, C02016, doi:10.1029/2007JC004371.

Jing, Z., and L. Wu (2014), Intensified diapycnal mixing in the midlatitude western boundary currents, *Sci. Rep.*, *4*, 7412.

Kunze, E. (1985), Near-inertial wave propagation in geostrophic shear, *J. Phys. Oceanogr.*, *15*, 544–565.

McGillicuddy, D. J. (2015), Formation of intrathermocline lenses by eddy-wind interaction, *J. Phys. Oceanogr.*, *45*, 606–612.

McGillicuddy, D. J., A. R. Robinson, D. A. Siegel, H. W. Jannasch, R. Johnson, T. D. Dickey, J. McNeil, A. F. Michaels, and A. H. Knap (1998), New evidence for the impact of mesoscale eddies on biogeochemical cycling in the Sargasso Sea, *Nature*, *394*, 263–266.

Munday, D. R., and X. Zhai (2015), Sensitivity of Southern Ocean circulation to wind stress changes: Role of relative wind stress, *Ocean Modell.*, *95*, 15–24.

Nikurashin, M., G. K. Vallis, and A. Adcroft (2012), Routes to energy dissipation for geostrophic flows in the Southern Ocean, *Nat. Geosci.*, *6*, 48–51.

Risien, C. M., and D. B. Chelton (2008), A global climatology of surface wind and wind stress fields from eight years of QuikSCAT scatterometer data, *J. Phys. Oceanogr.*, *38*, 2379–2413.

Scott, R., and Y. Xu (2009), An update on the wind power input to the surface geostrophic flow of the world ocean, *Deep-Sea Res. Pt I*, *56*, 295–304.

Song, H., J. Marshall, P. Gaube, and D. J. McGillicuddy (2015), Anomalous anthropogenic gas uptake by mesoscale eddies in the Southern Ocean, *J. Geophys. Res.*, *120*, 1065–1078.

Wunsch, C. (1998), The work done by the wind on the oceanic general circulation, *J. Phys. Oceanogr.*, *28*, 2332–2340.

Xu, C., X. D. Shang, and R. X. Huang (2014), Horizontal eddy energy flux in the world oceans diagnosed from altimetry data, *Sci. Rep.*, *4*, 5316.

Zhai, X., and R. J. Greatbatch (2007), Wind work in a model of the northwest Atlantic Ocean, *Geophys. Res. Lett.*, *34*, L04606, doi:10.1029/2006GL028907.

Zhai, X., R. J. Greatbatch, and J. Zhao (2005), Enhanced vertical propagation of storm-induced near-inertial energy in an eddying ocean channel model, *Geophys. Res. Lett.*, *32*, L18602, doi:10.1029/2005GL023643.

Zhai, X., H. L. Johnson, and D. P. Marshall (2010), Significant sink of ocean-eddy energy near western boundaries, *Nat. Geosci.*, *3*, 608–612.

Zhai, X., H. L. Johnson, D. P. Marshall, and C. Wunsch (2012), On the wind power input to the ocean general circulation, *J. Phys. Oceanogr.*, *42*, 1357–1365, doi:10.1175/JPO-D-12-09.1.